In-Beam Analysis for Multiple Uplinks per Antenna (MUPA) Using a 34-m Antenna

David D. Morabito,* Douglas S. Abraham,† David Heckman,* Marc Sanchez Net,* and Shan Malhotra‡

ABSTRACT. — The number of spacecraft that require support from NASA's Deep Space Network (DSN) is expected to increase significantly within the next few years. Thus, NASA has been exploring ways to increase capacity using existing antennas. One solution is beam-sharing. While successfully employed for simultaneous downlink, beam-sharing for simultaneous uplink using the same frequency band has not been an option. An approach to achieving near-simultaneous uplink involves multiplexing the data streams intended for all of the participating in-beam spacecraft onto a single uplink frequency. Here we focus on examining the various near-Earth and interplanetary scenarios involving multiple spacecraft and inspect the number of spacecraft that may fall within the beamwidth of a 34-m-diameter DSN station. The scenarios we examine include planetary orbital spacecraft, the Sun–Earth Lagrange points at L1 (SEL-1) and L2 (SEL-2), the lunar vicinity, and Gateway. For this study, we consider cases involving S-band (2 GHz), X-band (7.1–8.4 GHz), K-band (22–27 GHz), and Ka-band (32–34 GHz).

I. Introduction

The number of spacecraft that require support from NASA's Deep Space Network (DSN) is expected to increase significantly within the next few years. Key drivers include increasing reliance on more affordable, targeted SmallSat missions, a more robust science program, and the emergence of multielement human lunar exploration missions [1]. The projected increase in the number of antennas that will be needed to communicate with all of these missions is likely to be prohibitively expensive [1]. Thus, NASA has been exploring ways to increase capacity using existing antennas. One approach is beam-sharing. While successfully employed for simultaneous downlink, beam-sharing for simultaneous uplink using the same frequency band has not been an option.

An approach to achieving near-simultaneous uplink involves multiplexing the data streams intended for all participating in-beam spacecraft onto a single uplink frequency.

* Communications Architectures and Research Section.

† Formerly with the Customer Interface Management Office (retired).

‡ Planning and Execution Systems Section.

The research described in this publication was carried out by the Jet Propulsion Laboratory, California Institute of Technology, under a contract with the National Aeronautics and Space Administration (80NM0018D0004).

Each spacecraft then identifies which of the transfer frames is intended for it based on a spacecraft identification code. Known as multiple uplinks per antenna (MUPA), this technique has been under study for several years; now, key components are being prototyped, paths to implementation are being found, requirements are being defined, and ground and flight demonstrations are being pursued [1–4].

This paper focuses on the various near-Earth and interplanetary scenarios in which multiple spacecraft are involved. It examines the number of spacecraft that may fall within the beamwidth of the DSN station, given the various orbits and trajectories about a planet, in the lunar vicinity, at SEL-1 and SEL-2, and at Gateway. We define beamwidth limits as usually 3 dB (end-to-end half-power beamwidths [HPBW]). In some cases, we also consider a 10-dB down beamwidth, such as in the lunar vicinity. For this study, we consider cases involving the following frequency bands: S-band (2 GHz), X-band (7.1–8.4 GHz), K-band (22–27 GHz) and Ka-band (32–34 GHz).

II. Approach

We assemble the various orbital parameters or trajectory files and perform animations using the Satellite Orbital Analysis Program (SOAP) [5] to examine the various scenarios against the projected beams of the ground antenna. SOAP was used to generate snapshots of various orbital scenarios that we can examine against beamwidth (e.g., such as at a planet at different range distances). SOAP was also used to generate a report file consisting of various parameters, such as range distance and angle between spacecraft and planet center.

We also make use of the Beam Intercept Planning System (BIPS), an application developed for computing all of the motions of the spacecraft systems, communications ground stations, and possible occulting bodies (Mars, the Moon, etc.), then use this information to accurately identify the intervals of time when opportunities for multiple spacecraft per antenna (MSPA) and MUPA exist. BIPS computes all of the beamwidth-dependent opportunity intervals using trajectory models and can also supply statistical information about the collection of opportunities that exist in any scenario. It has several graphical and animation features that greatly help us visualize and understand the motions of the objects, visibility and beam constraints, and how these factors combine to impact potential MUPA opportunities.

III. Scenarios

In this section, we consider the various beam analysis scenarios, which include planetary (Section III.A), SEL-1 and SEL-2 (Section III.B), lunar and lunar vicinity (Section III.C), and Gateway direct-to-Earth (Section III.D). Table 1 depicts the various frequency bands and beamwidths for a 34-m DSN beam-waveguide (BWG) antenna for deep space frequency allocations, such as those used in the various planetary scenarios. Table 2 depicts the various frequency bands and beamwidths for a 34-m BWG antenna for near-Earth allocations, such as those used for lunar, SEL-1 and SEL-2, and Gateway scenarios. The

frequencies specified are center frequencies of each band and were obtained from DSN 810-005 documentation [6].

The end-to-end HPBW in Tables 1 and 2 were calculated using the formula BW = 1.1 λ/d (radians), where λ is the wavelength and d is the diameter of the antenna. These were then converted to units of mdeg by multiplying by $1{,}000*180/\pi$, and they match exactly with those provided in the 810-005 document [6].

Table 1. 34-m antenna beamwidths for deep space allocations.

Frequency Band	Uplink Frequency (GHz)	Uplink Beamwidth (mdeg)	Downlink Frequency (GHz)	Downlink Beamwidth (mdeg)
S-band	2.115	263	2.295	242
X-band	7.15	78	8.4	66
Ka-band	34.45	16	32	17

Table 2. 34-m antenna beamwidths for near-Earth allocations.

Frequency Band	Uplink Frequency (GHz)	Uplink Beamwidth (mdeg)	Downlink Frequency (GHz)	Downlink Beamwidth (mdeg)
S-band	2.0675	269	2.245	247
X-band	7.2125	77	8.475	66
K-band	22.85	24	26.25	21

A. Planetary Scenarios

Here we will consider four key planetary scenarios: Venus (Section III.A.1), Mars (Section III.A.2), Jupiter (Section III.A.3), and Saturn (Section III.A.4). Planets not considered at this time are interior planet Mercury and outer planets Uranus and Neptune. Usually, the outer planets are so far distant that most, if not all, orbiters or flyby trajectories would fall within the beamwidths of the DSN antennas at the applicable frequency bands.

1. Venus

For the case of the planet Venus, we consider the beamwidths for a 34-m BWG antenna at the nearest Earth–Venus distance (0.24 AU), at a 1 AU distance, and at the farthest Earth–Venus distance (1.74 AU). Shown in Table 3a are the three cases of planetary distance (in AU), the angular extent of the planet as seen from Earth (in mdeg), and the uplink beamwidth (in terms of number of planetary diameters) for S-band, X-band, and Ka-band. Table 3b displays the same information for the case of downlink.

Figures 1 and 2 include the orbit of the Venus Emissivity, Radio Science, InSAR, Topography, and Spectroscopy (VERITAS) spacecraft. The VERITAS spacecraft has a Science Phase I, when it is placed in a 6.1-hr orbit with polar inclination and a Science Phase II, when it goes into a 91-min orbit with a polar inclination at a 217-km altitude [7]. Also

Table 3a. Uplink HPBWs for Venus.

Planet Distance (AU)	Planet Ang Extent (mdeg)	S-band Beamwidth / Venus Diameters	X-band Beamwidth / Venus Diameters	Ka-band Beamwidth / Venus Diameters
0.24	19.26	14	4.03	0.84
1.00	4.64	57	17	3.48
1.74	2.66	99	29	6.08

Table 3b. Downlink HPBWs for Venus.

Planet Distance (AU)	Planet Ang Extent (mdeg)	S-band Beamwidth / Venus Diameters	X-band Beamwidth / Venus Diameters	Ka-band Beamwidth / Venus Diameters
0.24	19.26	13	3.43	0.90
1.00	4.64	52	14.24	3.74
1.74	2.66	91	24.84	6.53

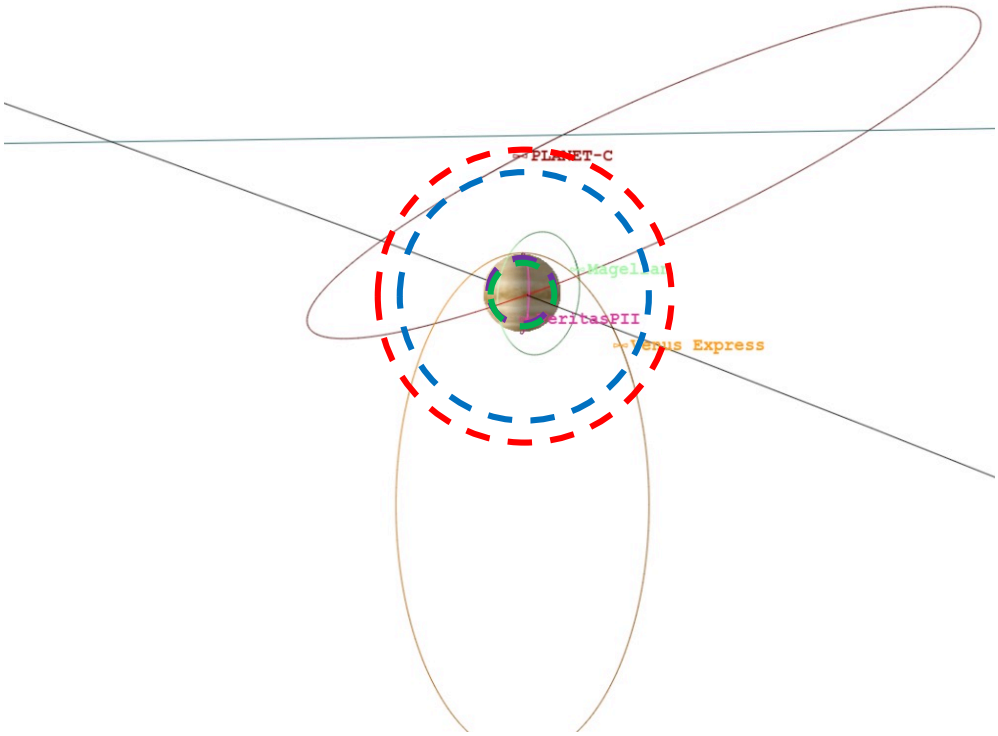

Figure 1. 34-m beamwidths at nearest Venus distance; X-band uplink (dashed red), X-band downlink (dashed blue), Ka-band downlink (dashed purple), and Ka-band uplink (dashed green).

shown in Figures 1 and 2 is the orbit for the ESA Venus Express (VEX) mission [8]. Other spacecraft to be considered in later phases of this study include Deep Atmosphere Venus Investigation of Noble gases, Chemistry, and Imaging (DAVINCI) and Rocket Lab's Venus mission. DAVINCI involves a flyby spacecraft and an in situ atmospheric probe to study Venus, and it has a 2031–2032 scheduled launch date [9, 9b]. Rocket Lab is likely to be the first private mission to Venus, where it will search for possible evidence of organic

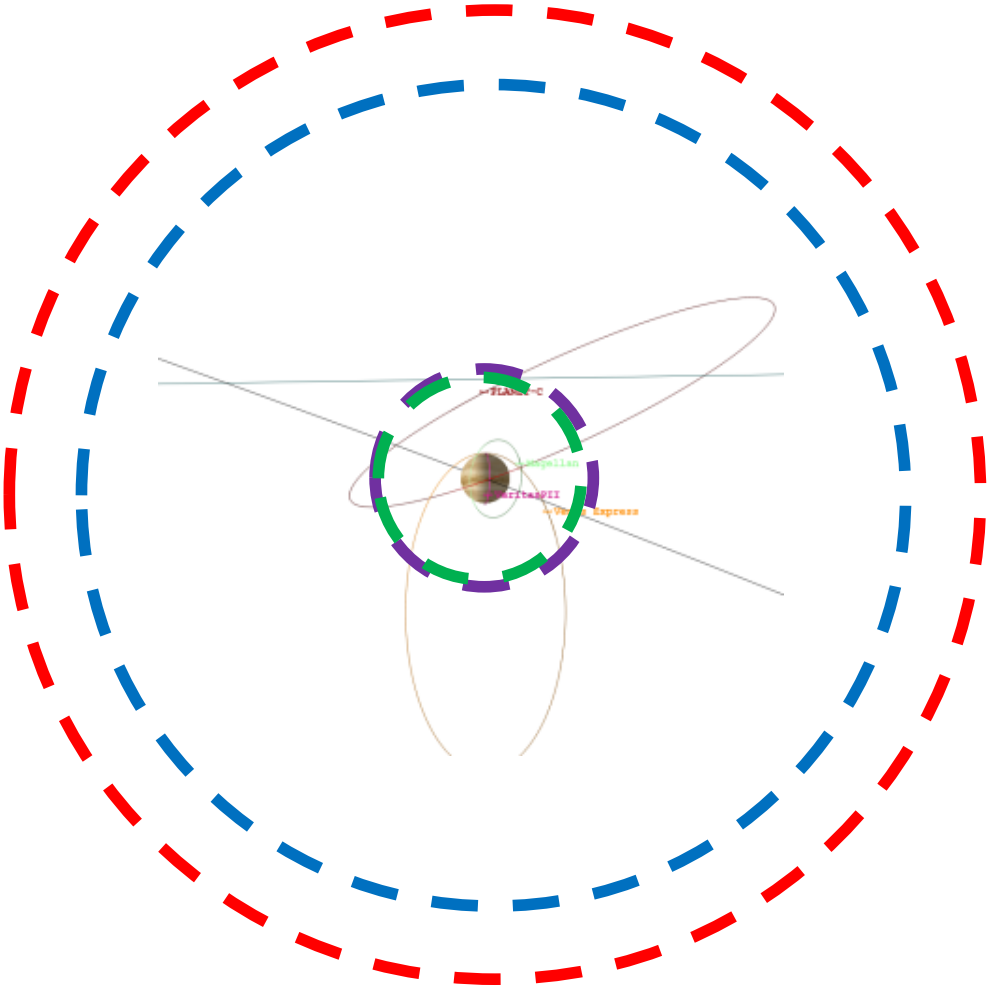

Figure 2. 34-m beamwidths at farthest Venus distance; X-band uplink (dashed red), X-band downlink (dashed blue), Ka-band downlink (dashed purple), and Ka-band uplink (dashed green).

compounds in the Venusian clouds. It will make use of an Electron launch vehicle and Photon spacecraft, and it will send a probe to an altitude of about 30 miles, where the atmospheric conditions are similar to those at Earth [10,11].

Figure 1 displays a SOAP snapshot of the planet Venus, along with 34-m HPBWs for the deep space frequency bands of interest at the nearest Earth–Venus distance: X-band uplink (dashed red), X-band downlink (dashed blue), Ka-band uplink (dashed green), and Ka-band downlink (dashed purple). Also shown are sample planetary orbits for Magellan (now defunct), VERITAS (Phase II), VEX, and Planet C. The X-band HPBWs (when centered on Venus) can accommodate any surface/balloon/aerobot assets in view as well as low-altitude "circular" orbiters. In some cases, however, portions of a highly eccentric orbit may lie outside the X-band beam of the MUPA antenna; for example, see Planet C and VEX orbits in Figure 1. The Ka-band beam is effectively comparable to the planet's angular diameter at the closest Earth–Venus distance and should be able to accommodate any surface vehicles, balloons, and portions of very low-altitude orbits.

Figure 2 displays a SOAP snapshot of the planet Venus along with 34-m HPBWs for the deep space frequency bands of interest at the farthest Earth–Venus distance: X-band uplink (dashed red), X-band downlink (dashed blue), Ka-band uplink (dashed green), and Ka-band downlink (dashed purple). Also shown are sample spacecraft orbits for Magellan (no longer functioning), VERITAS (future orbiter), VEX, and Planet C. Other future missions include DAVINCI and EnVision. The X-band HPBWs should be able to accommodate any surface/balloon/aerobot assets in view as well as all orbiters, including those shown with very elongated eccentricities. The Ka-band beam accommodates any surface vehicles, aerobots, or balloons in view and all low-altitude orbiters. There are periods when portions of very elongated orbits fall outside the Ka-band beam.

Link considerations include accounting for a 3-dB worst-case loss due to the extremity of the HPBW as well as accounting for increased hot body noise when the ground antenna beam is pointed at the center of the planet. Hot body noise temperature estimates at X-band for a 34-m antenna pointed at Venus-center are 22.9 K at the closest Venus–Earth range distance and 0.6 K at the farthest range distance. Hot body noise estimates at Ka-band for a 34-m antenna pointed at Venus-center are 191.3 K at the closest Venus–Earth range distance and 4.8 K at the farthest range distance. The hot body noise estimates presented here are based on data and formulation provided in the DSN 810-005 document [12].

Even missions with highly elliptical orbits spend a significant amount of time in beam (e.g., Planet C). SOAP was set up to generate a report file consisting of Earth–Venus range distance and the angle between the "Planet C" spacecraft and Venus-center as seen from Earth. The report file was imported into Microsoft Excel. Figure 3 displays a plot containing the output of the report file for the case of a spacecraft with a highly elliptical orbit that sometimes extends beyond the beamwidth of the DSN ground station's X-band beam. The angle between Planet C and Venus is shown in blue, and the X-band HPBW/2 beamwidth limit is shown in red, as seen from Earth. We assume that the 34-m beam is pointed at Venus-center, with an uplink HPBW of 78 mdeg at X-band, thus HPBW/2 = 39 mdeg (red line in Figure 3). The small signatures and dips around days 10.5 and 21.5 occur when the spacecraft is aligned with Venus-center. For this sample period,

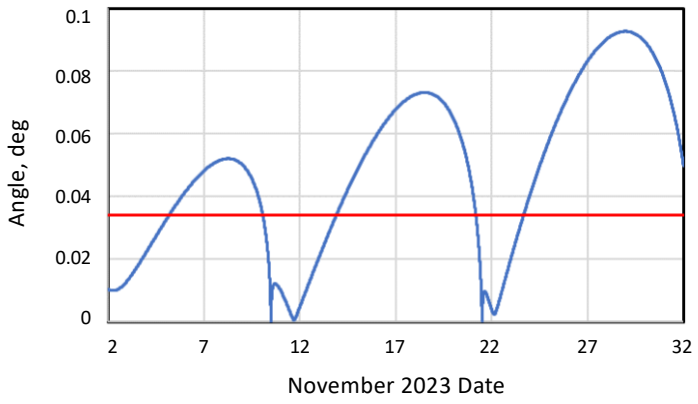

Figure 3. Angle between Planet C and Venus-center as a function of time (blue). Also shown is the HPBW/2 limit of the X-band uplink beam (red). Note that day 31 is actually December 1.

there are 10.9 days when the angle lies below the uplink HPBW/2. Thus, over the full 30 days of the trajectory shown (November 2 to December 1), Planet C could participate in a MUPA session 36.5% of the time when the 34-m is pointed at Venus-center (31.6% for downlink MSPA). Although Planet C was in front of the planet during the two occurrences about halfway through the month, the algorithm can be modified to adjust or account for cases of spacecraft occultation by the planet, but the net result difference will be small.

2. Mars

For the case of the planet Mars, we consider the beamwidths for a 34-m BWG antenna at the nearest Earth–Mars distance (0.374 AU), a 1 AU distance, and the farthest Earth–Mars distance (2.675 AU). Shown in Table 4a are the three cases of planetary distance (in AU), the angular extent of the planet as seen from Earth (in mdeg), and the uplink beamwidth (in terms of number of planetary diameters) for S-band, X-band, and Ka-band. Table 4b displays the same information for the case of downlink. Table 1 displays the relevant center frequencies of each deep space band, along with the uplink and downlink frequencies and angular HPBWs.

Table 4a. Uplink HPBWs for Mars.

Planet Distance (AU)	Planet Ang Extent (mdeg)	S-band Beamwidth / Mars Diameters	X-band Beamwidth / Mars Diameters	Ka-band Beamwidth / Mars Diameters
0.374	6.94	38	11	2.3
1	2.60	101	30	6.2
2.675	0.97	271	80	16.6

Table 4b. Downlink HPBWs for Mars.

Planet Distance (AU)	Planet Ang Extent (mdeg)	S-band Beamwidth / Mars Diameters	X-band Beamwidth / Mars Diameters	Ka-band Beamwidth / Mars Diameters
0.374	6.94	35	10	2.5
1	2.60	93	25	6.7
2.675	0.97	250	68	17.9

Figure 4 displays a SOAP snapshot of the planet Mars along with 34-m HPBWs for the deep space frequency bands of interest at the nearest Earth–Mars distance: X-band uplink (dashed red), X-band downlink (dashed blue), Ka-band uplink (dashed green), and Ka-band downlink (dashed purple). Also shown are sample planetary orbits for various past and present spacecraft and those of the moons Phobos and Deimos. The X-band HPBWs should be able to accommodate any surface/balloon/aerobot assets in view as well as all of the shown orbiters, except for a small fraction of the highly elliptical orbit for the Mars Orbiter Mission (MOM). The Ka-band beams would accommodate all visible surface assets, balloons, and aerobots as well as the lowest-altitude orbiters and various fractions of highly elliptical orbits. The orbit for Mars Reconnaissance Orbiter (MRO) (~400 km altitude) is difficult to discern on Figure 4 because it lies very close to the planet on this scale.

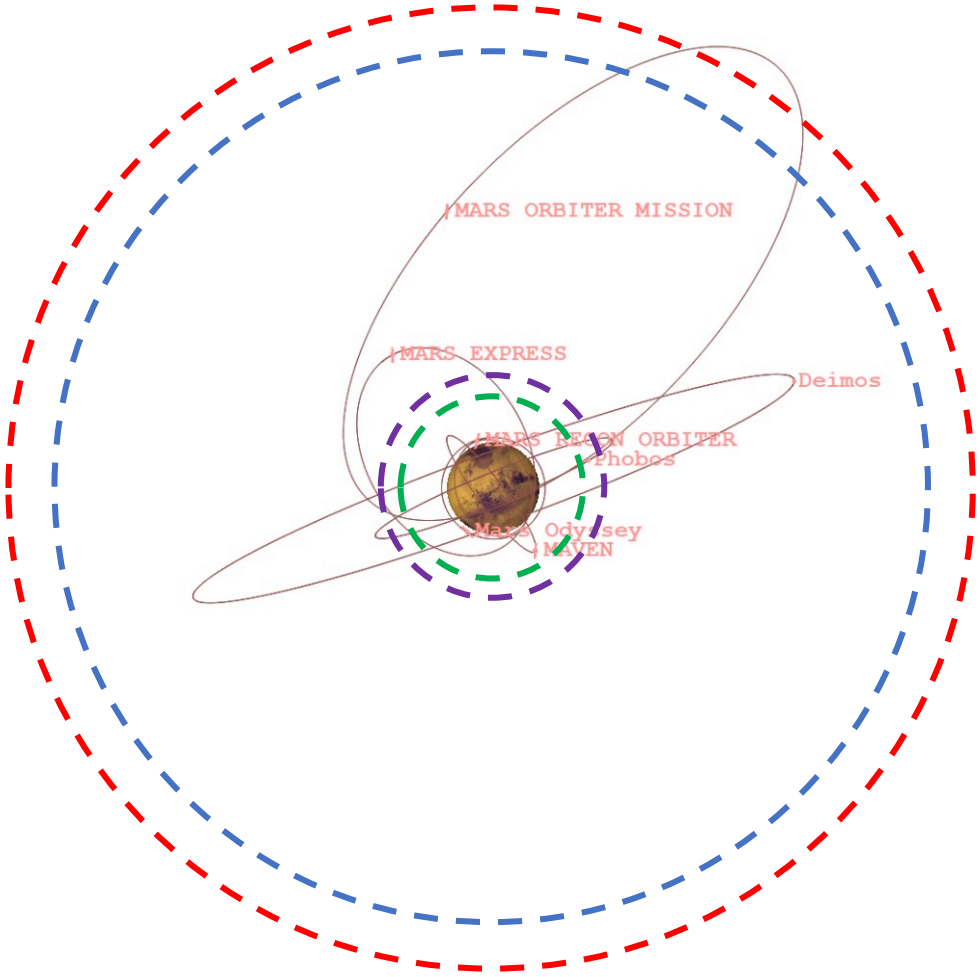

Figure 4. Beamwidths nearest Earth–Mars distance, along with SOAP snapshot of Mars with orbits of Phobos and Deimos and selected spacecraft; X-band uplink (dashed red), X-band downlink (dashed blue), Ka-band downlink (dashed purple), and Ka-band uplink (dashed green).

Figure 5 displays a SOAP snapshot of the planet Mars along with 34-m HPBWs for the deep space frequency bands of interest at the farthest Earth–Mars distance: X-band uplink (dashed red), X-band downlink (dashed blue), Ka-band uplink (dashed green), and Ka-band downlink (dashed purple). Also shown are orbits for available spacecraft trajectories. The X-band HPBWs should be able to accommodate any surface/balloon/aerobot assets in view as well as all shown orbiters, including those with very elongated eccentricities. The Ka-band beam accommodates any surface vehicles, aerobots, or balloons in view and all spacecraft with orbits out to an altitude of ~53,000 km.

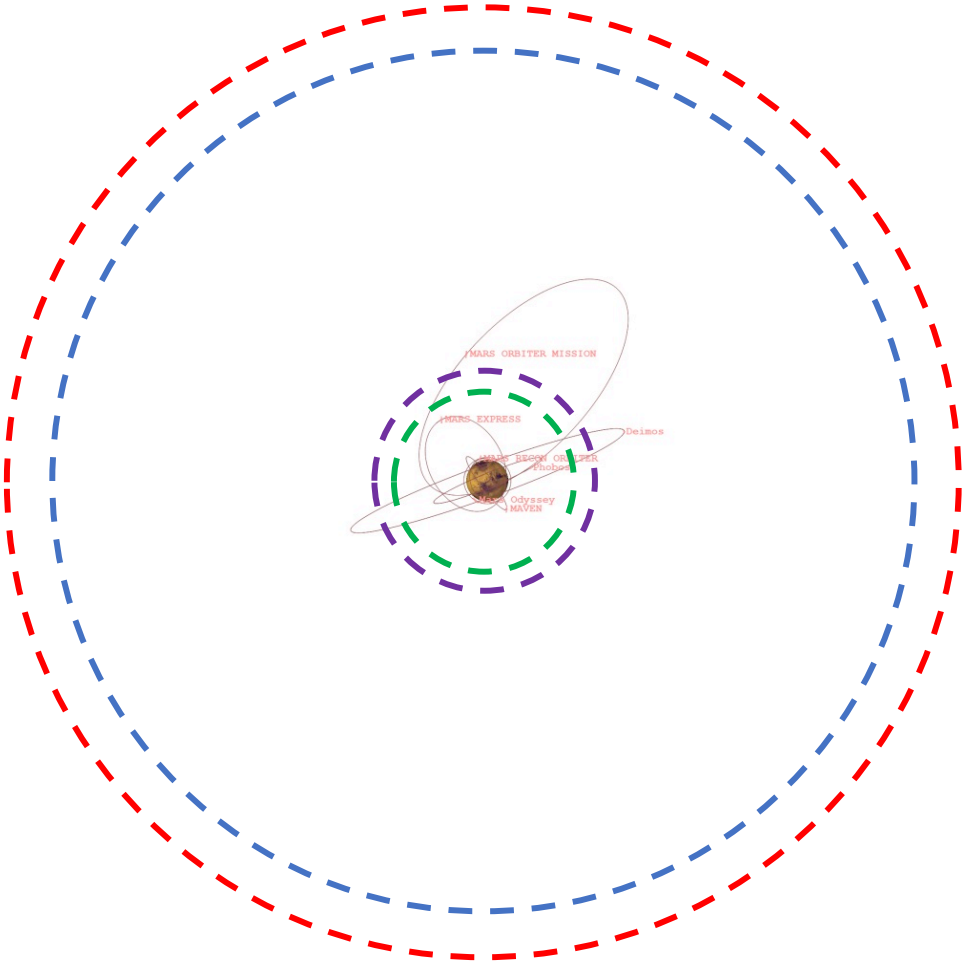

Figure 5. Beamwidths at farthest Earth–Mars distance, along with SOAP snapshot of Mars with orbits of Phobos and Deimos and selected spacecraft; X-band uplink (dashed red), X-band downlink (dashed blue), Ka-band downlink (dashed purple), and Ka-band uplink (dashed green).

The Escape and Plasma Acceleration and Dynamics Explorers (EscaPADE) mission involves two spacecraft that will orbit Mars and study ion and sputtered-particle escape from the Martian ionosphere and atmosphere [13]. It is expected to possibly launch in 2024 and conduct its active mission from August 2025 to March 2027. Figure 6 shows the case when the two EscaPADE spacecraft are in orbit around Mars at maximum Earth–Mars distance. All of the spacecraft easily fall within the X-band and Ka-band beams at this time. (Also shown are the orbits of Mars' two moons Phobos and Deimos.) Based on an earlier study, both EscaPADE spacecraft are demonstrated to be within the MSPA beam for ~65% of the trip out to Mars [13]. We find that the two spacecraft are simultaneously available for MUPA operations about 66% of the time once they are at Mars, based on a BIPS analysis. Table 5 displays the MUPA in-beam statistics for the three DSN sites as well as those for the overall network while the two EscaPADE spacecraft are in their operational phase at Mars from August 14, 2025, to March 4, 2027. The network availability fraction is not 100% because of periods of occultation when one or both spacecraft lie behind the planet and gaps in station visibility. Gaps can occur, for example, during crossovers between sites

when the planet is not visible at both sites, such as when it is lying below the 10-deg elevation angle mask used for uplink operations, as the DSN cannot transmit below a 10-deg elevation angle. The above analysis applies to EscaPADE's X-band frequency allocation.

Table 5. EscaPADE in-beam statistics.

Site	Time Fraction Available %
Goldstone	29.66
Canberra	26.78
Madrid	29.51
Network	65.94

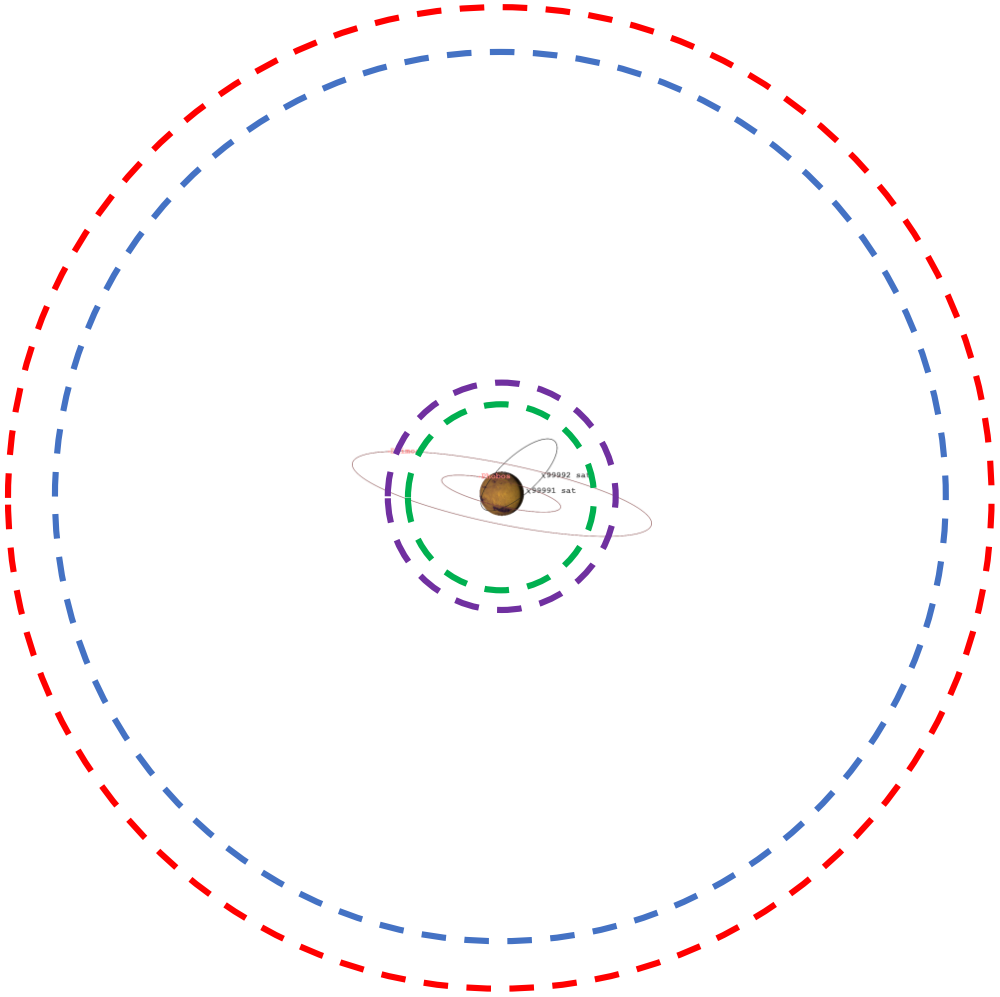

Figure 6. SOAP snapshot of orbits of two EscaPADE spacecraft (99991 and 99992) at maximum Earth–Mars distance; X-band uplink (dashed red), X-band downlink (dashed blue), Ka-band downlink (dashed purple), and Ka-band uplink (dashed green).

3. Jupiter

For the case of the planet Jupiter, we consider the beamwidths for a 34-m BWG antenna at the nearest Earth–Jupiter distance (4.2 AU), a 5 AU intermediate distance, and the farthest Earth–Jupiter distance (6.2 AU). Shown in Table 6a are the three cases of planetary distance (in AU), the angular extent of the planet as seen from Earth (in mdeg), and the uplink beamwidth (in terms of number of planetary diameters) for S-band, X-band, and Ka-band.

Table 6b displays the same information for the case of downlink. Table 1 displays the relevant center frequencies of each deep space band, along with the uplink and downlink frequencies and angular HPBWs.

Table 6a. Uplink HPBWs for Jupiter.

Planet Distance (AU)	Planet Ang Extent (mdeg)	S-band Beamwidth / Jupiter Diameters	X-band Beamwidth / Jupiter Diameters	Ka-band Beamwidth / Jupiter Diameters
4.20	13.03	20	5.97	1.24
5.00	10.95	24	7.10	1.47
6.20	8.83	30	8.81	1.83

Table 6b. Downlink HPBWs for Jupiter.

Planet Distance (AU)	Planet Ang Extent (mdeg)	S-band Beamwidth / Jupiter Diameters	X-band Beamwidth / Jupiter Diameters	Ka-band Beamwidth / Jupiter Diameters
4.20	13.03	19	5.08	1.33
5.00	10.95	22	6.04	1.59
6.20	8.83	27	7.50	1.97

Figure 7 displays a SOAP snapshot of the planet Jupiter along with 34-m HPBWs for the deep space frequency bands of interest at the nearest Earth–Jupiter distance: X-band uplink (dashed red), X-band downlink (dashed blue), Ka-band uplink (dashed green), and Ka-band downlink (dashed purple). Also shown are sample planetary orbits for various spacecraft. The X-band HPBWs should be able to accommodate any balloon or aerobot assets in view. The Ka-band beam would accommodate all visible balloon or aerobot assets as well as the orbiters with low altitudes. Only portions of the Europa Clipper, JUpiter ICy

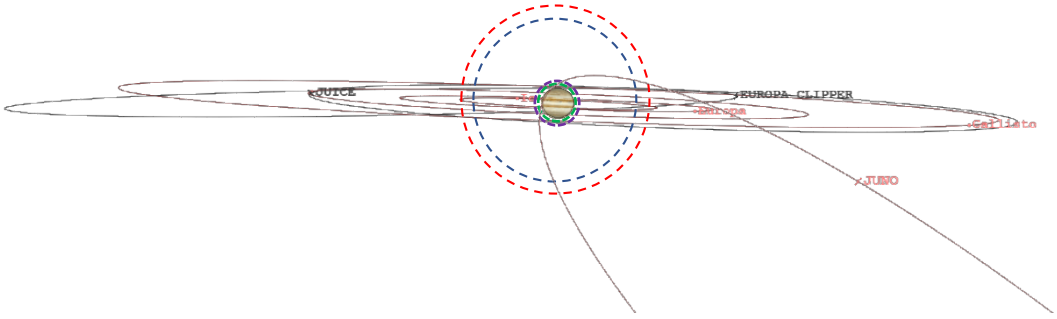

Figure 7. X-band and Ka-band beams superimposed with planet Jupiter and Galilean satellite orbits at nearest Earth–Jupiter range distance—SOAP depiction; X-band uplink (dashed red), X-band downlink (dashed blue), Ka-band downlink (dashed purple), and Ka-band uplink (dashed green). The available Juno trajectory is referenced to 2022 while that for Europa Clipper is for 2031. Since the two available spacecraft trajectories cannot show up at the same time, the Juno[1] SOAP snapshot was superimposed upon the Europa Clipper SOAP snapshot. Note that JUICE is in orbit around Ganymede, at this time.

[1] Juno is not in its designed trajectory. It was supposed to reduce to a much less eccentric 14-day orbit, but problems with helium valves that are important during main engine burns led to a decision to leave it in its highly eccentric 53-day orbit.

moons Explorer (JUICE), and Juno orbits will be covered if the 34-m antenna beam is pointed at Jupiter-center. With regard to low-altitude circular orbiters, radiation may drive survivability; however, there could be cases in which orbits may be low enough to lie beneath the radiation belts.

Figure 8 displays a SOAP snapshot of the planet Jupiter along with 34-m HPBWs for the deep space frequency bands of interest at the farthest Earth–Jupiter distance: X-band uplink (dashed red), X-band downlink (dashed blue), Ka-band uplink (dashed green), and Ka-band downlink (dashed purple). Also shown are sample spacecraft orbits for available spacecraft trajectories. The X-band HPBWs should be able to accommodate any balloon or aerobot assets in view as well as portions of spacecraft orbits that may impinge inside any of the beams when the ground antenna is pointed at Jupiter-center. The Ka-band beam accommodates any aerobots or balloons in view and portions of spacecraft orbits that may impinge inside any of the beams.

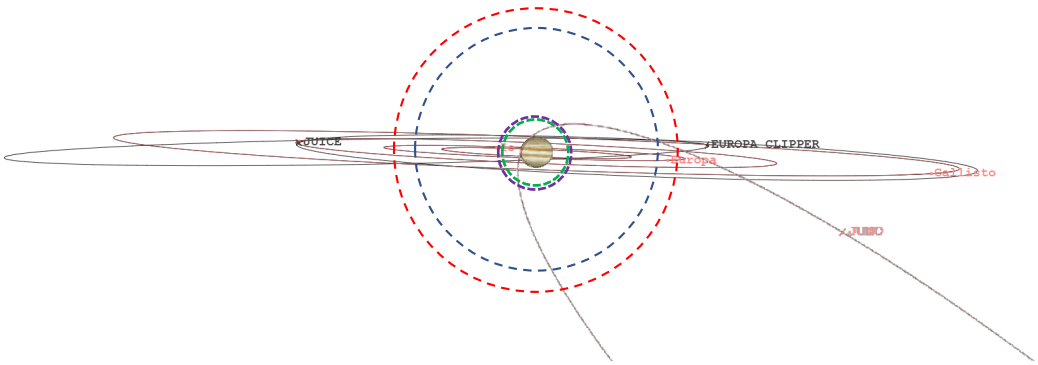

Figure 8. Beamwidths at farthest Earth–Jupiter distance, centered on Jupiter; X-band uplink (dashed red), X-band downlink (dashed blue), Ka-band downlink (dashed purple), and Ka-band uplink (dashed green). Note that JUICE is in orbit around Ganymede, at this time.

Figure 9 displays a SOAP snapshot of the planet Jupiter along with 34-m HPBWs for the deep space frequency bands of interest at the farthest Earth-Jupiter distance when the beam is centered on Europa Clipper: X-band uplink (dashed red), X-band downlink (dashed blue), Ka-band uplink (dashed green), and Ka-band downlink (dashed purple). Also shown are sample spacecraft orbits for available spacecraft trajectories.

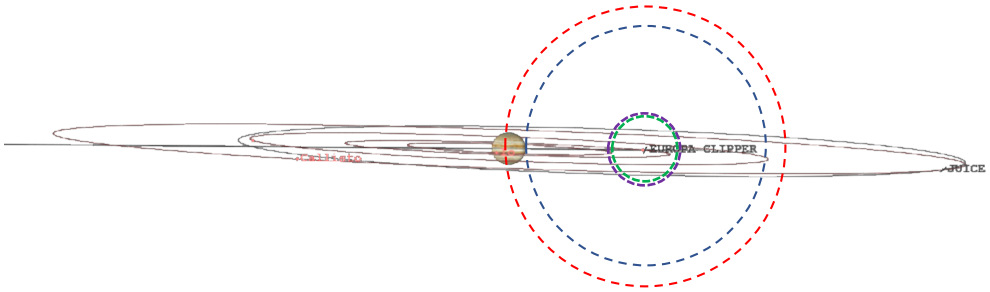

Figure 9. Beamwidths at farthest Jupiter distance—MUPA beam centered on Europa Clipper; X-band uplink (dashed red), X-band downlink (dashed blue), Ka-band downlink (dashed purple), and Ka-band uplink (dashed green). Note that Europa Clipper is at Europa and JUICE is at Ganymede.

An analysis of the in-beam common periods involving the Europa Clipper and JUICE spacecraft while at Jupiter was conducted to infer periods of MUPA opportunity at X-band. Figure 10 displays the angle between the two spacecraft (in blue) along with the HPBW/2 limit (in red) starting at the time JUICE arrives at Jupiter in late 2031 to the end of the common available trajectory data in September 2034.

Using the expected uplink X-band beamwidth of 0.078 deg for a 34-m antenna, while the boresight was pointed at one of the two spacecraft, the in-beam statistics over the period of February 1, 2032, to September 3, 2034, were evaluated as shown in Table 7. Here the percentage of common MUPA visibility was evaluated using output reports from both BIPS and SOAP for each of the three DSN sites as well as for the overall network. For the DSN sites, a minimum elevation angle of 10 deg was assumed. As shown in the table, very good agreement was achieved between the two programs. The slight differences would be due to the different configuration parameters of the individual program sets, such as specific DSN antenna assumed.

Table 7. Percentage of common visibility versus site for Europa Clipper / JUICE MUPA opportunities.

Site	BIPS %	SOAP %
Goldstone	5.28	5.26
Canberra	7.05	7.02
Madrid	5.09	5.11
Network	14.35	14.46

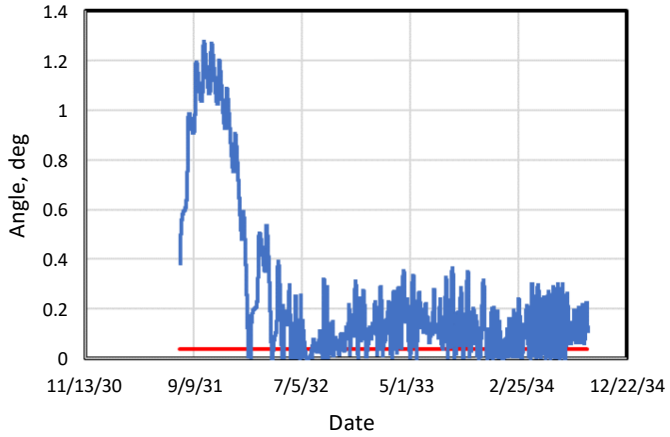

Figure 10. Angle between Europa Clipper and JUICE spacecraft (in blue) along with the HPBW/2 limit (in red) from JUICE arrival at Jupiter in July 2031 up to September 2034.

Upon inspection of Figure 10, one can see a high concentration of angles that lie below the HPBW/2 MUPA threshold. If we evaluate the statistics for this period from about August 2033 to September 2034, the overall network MUPA visibility percentage increases from 14.4% to 19.2%.

Link considerations involve the added hot body noise that would be encountered by the ground station antenna pattern against the planetary body. Hot body noise at X-band for a 34-m antenna pointed at Jupiter-center, would be 3.32 K at closest range and 1.47 K at farthest range distance. The added hot body noise at Ka-band for a 34-m antenna pointed at Jupiter-center would be 37.3 K at closest range distance and 17.1 K at farthest range distance. These estimates were obtained using the formulation provided in DSN document 810-005 [12].

4. Saturn

For the case of the planet Saturn, we consider the beamwidths for a 34-m BWG antenna at the nearest Earth–Saturn distance (8 AU), a 9 AU intermediate distance, and the farthest Earth–Saturn distance (11 AU). Shown in Table 8a are the three cases of planetary distance (in AU), the angular extent of the planet as seen from Earth (in mdeg), and the uplink beamwidth (in terms of number of planetary diameters) for S-band, X-band, and Ka-band. Table 8b displays the same information for the case of downlink. Table 1 displays the relevant center frequencies of each deep space band, along with the uplink and downlink frequencies and angular HPBWs.

Table 8a. Uplink HPBWs for Saturn.

Planet Distance (AU)	Planet Ang Extent (mdeg)	S-band Beamwidth / Saturn Diameters	X-band Beamwidth / Saturn Diameters	Ka-band Beamwidth / Saturn Diameters
8	5.55	47	14.01	2.91
9	4.95	53	15.70	3.26
11	4.05	65	19.19	3.98

Table 8b. Downlink HPBWs for Saturn.

Planet Distance (AU)	Planet Ang Extent (mdeg)	S-band Beamwidth / Saturn Diameters	X-band Beamwidth / Saturn Diameters	Ka-band Beamwidth / Saturn Diameters
8	5.55	44	11.92	3.13
9	4.95	49	13.36	3.51
11	4.05	60	16.33	4.29

Figure 11 displays a SOAP snapshot of the planet Saturn, along with 34-m HPBWs for the deep space frequency bands of interest at the nearest Earth–Saturn distance: X-band uplink (dashed red), X-band downlink (dashed blue), Ka-band uplink (dashed green), and Ka-band downlink (dashed purple). Also shown are sample planetary orbits for Saturn's moons Titan and Hyperion, and the Cassini spacecraft (now defunct). The X-band HPBWs should be able to accommodate any balloon/aerobot assets in view as well as portions of any spacecraft orbits that may fall within the beams. The Ka-band beam would accommodate all visible assets, balloons, or aerobots as well as any lower-altitude orbiters, if they can survive Saturn's environment for any length of time. Concerns with such orbits include prolonged radiation exposure or likelihood of colliding with ring elements. Most orbiters will likely involve very eccentric orbits, like Cassini's, and portions of any such orbit would lie outside the beamwidths of the 34-m antenna (if pointed at Saturn-center). Given a sample Cassini trajectory spanning from April 16, 2007, 12:00 UTC to May 5, 2007, 0:00 UTC (a 21.5-day span), it was found that Cassini would lie within an X-band uplink beamwidth centered on Saturn about 24.3% of the time (5.2 days).

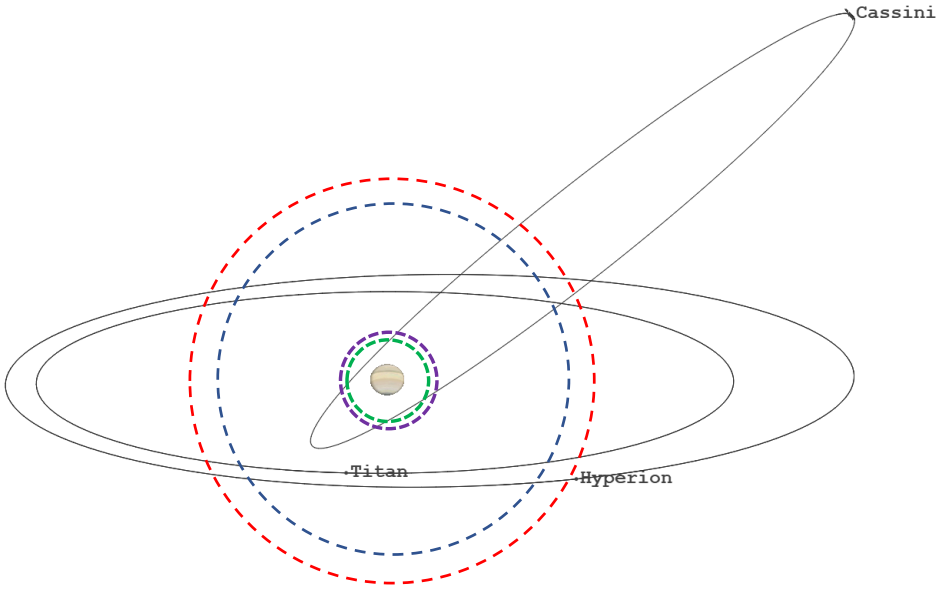

Figure 11. Beamwidths at nearest Saturn distance; X-band uplink (dashed red), X-band downlink (dashed blue), Ka-band downlink (dashed purple), and Ka-band uplink (dashed green).

B. Sun–Earth L1 and Sun–Earth L2 Scenarios

Here we present the MUPA beam analysis for cases involving SEL-1, situated about 0.01 AU from Earth toward the Sun, and SEL-2, situated about 0.01 AU behind Earth as viewed from the Sun. These locations allow for reasonably stable orbits for spacecraft in halo orbits about them.

At SEL-1, the spacecraft we have considered include Interstellar Mapping and Acceleration Probe (IMAP), Carruthers Geocorona Observatory (Carruthers), Near-Earth Object (NEO) Surveyor, Wind, Solar and Heliospheric Observatory (SOHO), Deep Space Climate Observatory (DSCOVR), and Advanced Composition Explorer (ACE). Trajectories were not yet available for Advanced Telescope for High Energy Astrophysics (ATHENA) and Space Weather Follow On-Lagrange 1 (SWFO-L1). At SEL-2, the spacecraft we have considered include the James Webb Space Telescope (JWST), Global Astrometric Interferometer for Astrophysics (GAIA), and Euclid. Trajectory files were not yet available for upcoming missions Nancy Grace Roman Space Telescope and Atmospheric Remote-sensing Infrared Exoplanet Large-survey (ARIEL). The dates of operation for each SEL-1 and SEL-2 spacecraft are tabulated in Table 9.

Figure 12 shows the location of the various Sun–Earth Lagrange points (not to scale). Superimposed on this diagram (in red) is an example of the range distance (R) to a hypothetical spacecraft on the L2 halo orbit, along with the subtended angle of one-half of the beamwidth $\theta/2$. The denoted distance X is thus the separation between any two spacecraft at that location, which would simultaneously lie within a MUPA beam centered on one spacecraft at the location. Thus, SOAP reports were generated whereby the resulting separations were logged and noted for the various frequency bands of interest.

Table 9. Dates of operation for each of the SEL-1 and SEL-2 spacecraft.

Location	Spacecraft	Dates of Operation		Comment
		From	To	
SEL-1	ACE	12/1/97	Present	
SEL-1	Wind	5/1/04	Present	
SEL-1	SOHO	5/1/96	Present	
SEL-1	DSCOVR	7/6/15	Present	
SEL-1	NEO Surveyor	9/1/27		Planned Launch
SEL-1	Carruthers	2025		Planned Launch
SEL-1	IMAP	5/1/25		Planned Launch
SEL-1	ATHENA (ESA-2037)	2035		Planned Launch
SEL-1	SWFO-L1	3/31/25		Planned Launch
SEL-2	GAIA (ESA)	1/8/24	Present	
SEL-2	JWST	7/12/22	Present	
SEL-2	Euclid (ESA)	8/1/23	Present	
SEL-2	Nancy Grace Roman Space Telescope	5/1/27		Planned Launch
SEL-2	ARIEL (ESA)	2029		Planned Launch

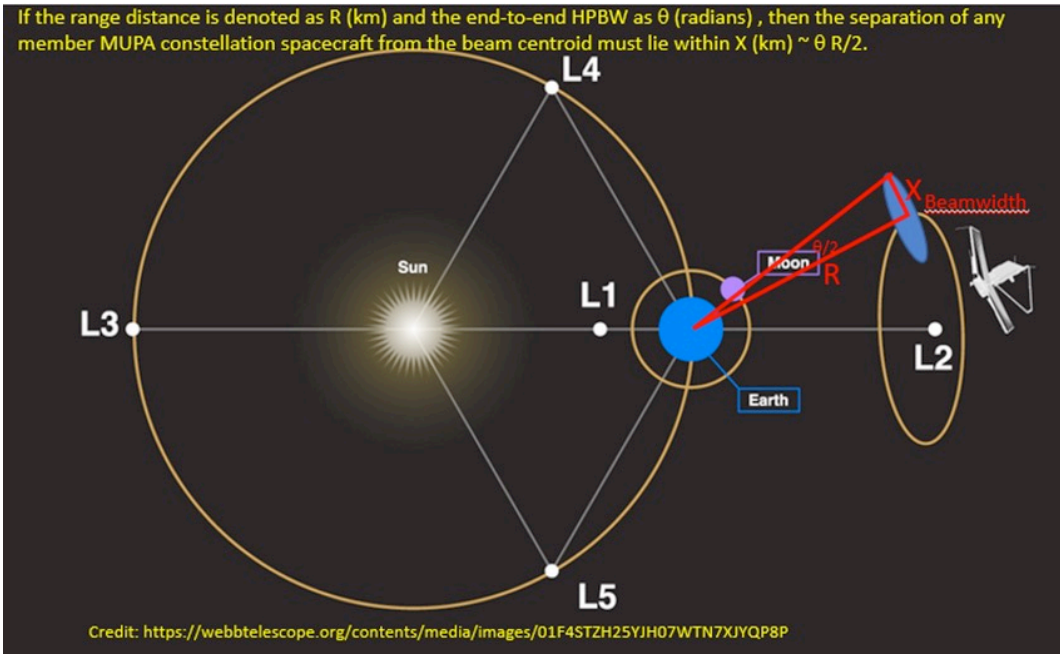

Figure 12. Example geometry of figuring out the separation between spacecraft at a Lagrange point, such as to lie within a selected beamwidth.

1. SEL-1 Beam Analysis

Figure 13 shows a SOAP snapshot of the Sun as seen from Earth, along with the seven L1 spacecraft in halo orbits around the Sun–Earth L1 point (Wind, SOHO, DSCOVR, ACE, NEO Surveyor, Carruthers, and IMAP), based on available trajectory files. Given that the

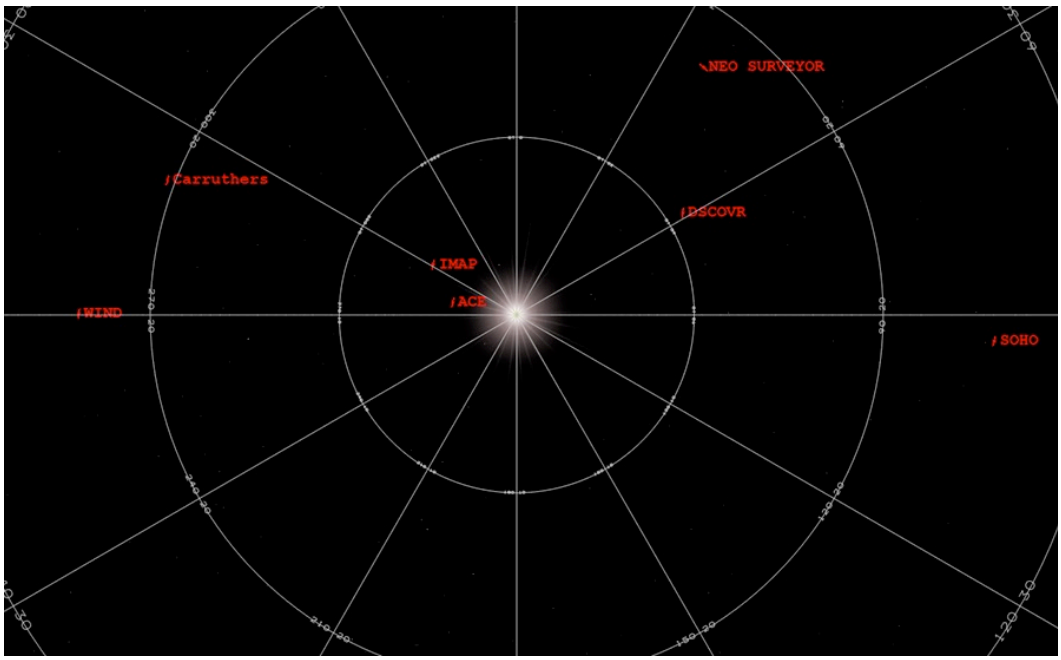

Figure 13. SOAP snapshot of view from Earth toward the Sun showing six spacecraft in halo orbits around SEL 1.

extent of the halo orbit as seen from Earth is on the order of ±25 deg, the chance of catching any two of these spacecraft within an X-band downlink beamwidth of 0.065 deg is very small. A constellation of spacecraft specifically designed to lie within an X-band beam at L1 would be a better scenario.

A SOAP animation was run over an approximate two-year period whereby the range distances from Earth to each of four SEL-1 spacecraft were output to a "report" file at one-day marks. Figure 14 illustrates how the permissible distance from the MUPA beam centroid would vary for a hypothetical MUPA constellation flying at each of the selected SEL-1 trajectories at the three uplink frequencies of interest over a 2022-to-2025 time period: S-band (a), X-band (b), and K-band (c). These are based on the beamwidths provided in Table 2, which specifies uplink and downlink center frequencies and corresponding beamwidths for the near-Earth allocations pertaining to the SEL-1 cases discussed here.

Table 10 lists the ranges of maximum separation between any two spacecraft for each band at SEL-1 inferred from Figure 14. See Figure 12 for an image illustrating the spacecraft separation needed to lie within a selected beamwidth at a Lagrange point.

Table 10. Ranges of maximum separation between any two member spacecraft for each band at L1.

Frequency Band	Separation Distance Range (km)
S-band	6,000 to 8,000
X-band	1,620 to 2,200
K-band	520 to 700

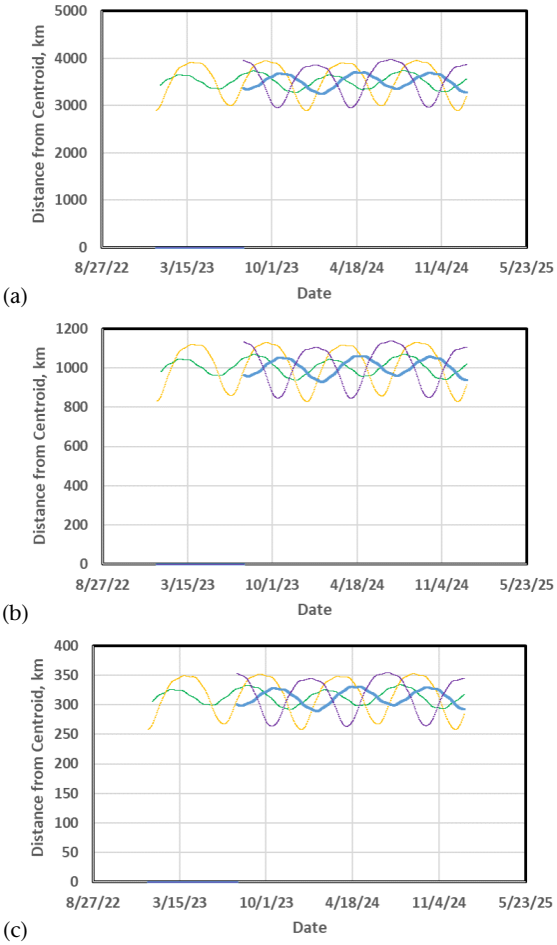

Figure 14. Permissible maximum separation between example L1 halo orbit spacecraft so as to reside inside the uplink beamwidths for S-band (a), X-band (b), and K-band (c).

Legend:
SOHO (yellow), ACE (green), DSCOVR (blue), and Wind (purple).

2. SEL-2 Beam Analysis

At SEL-2, the spacecraft we have considered include JWST, Euclid, Nancy Grace Roman Space Telescope (2027), and ARIEL (ESA-2029). Figure 15 shows a SOAP snapshot of the spacecraft in halo orbits around the Sun–Earth L2 point as seen from the Sun looking toward Earth (using JWST as the centered reference platform). Note that Nancy Grace Roman Space Telescope would be flying in place of JWST.

An animation was run over an approximate two-year period whereby the distances from Earth to each of the three spacecraft were output to a report file at one-day marks. The three plots in Figure 16 illustrate how the distance from the MUPA beam centroid would vary for a hypothetical MUPA constellation flying at the various SEL-2 trajectories for the three uplink frequencies: S-band (a), X-band (b), and K-band (c), based on the beamwidths provided in Table 2. Table 11 lists the ranges of maximum separation between any two spacecraft for each band at L2 inferred from Figure 16.

Table 11. Ranges of maximum separation between any two member spacecraft for each band at L2.

Frequency Band	Separation Distance Range (km)
S-band	6,000 to 8,000
X-band	1,620 to 2,200
K-band	520 to 700

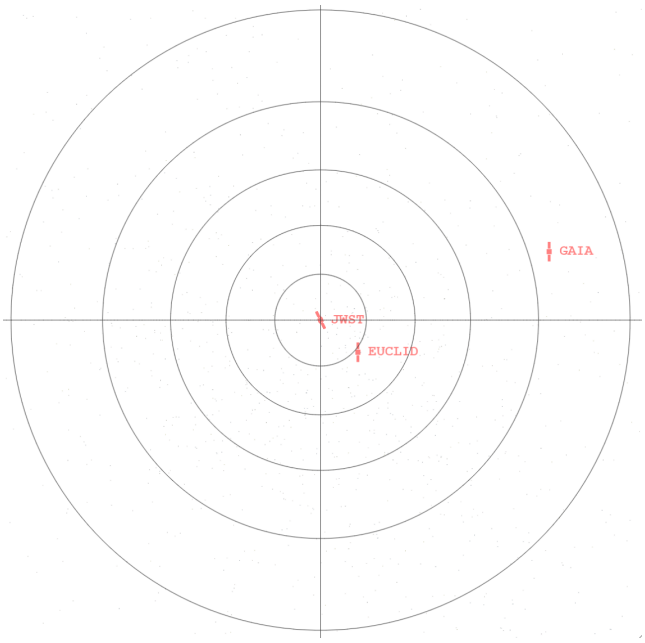

Figure 15. SOAP snapshot of view from Earth toward the Sun in the vicinity of SEL-2 showing spacecraft currently in halo orbits (using JWST as the boresight reference). Cone angle circle markers are 10 deg apart.

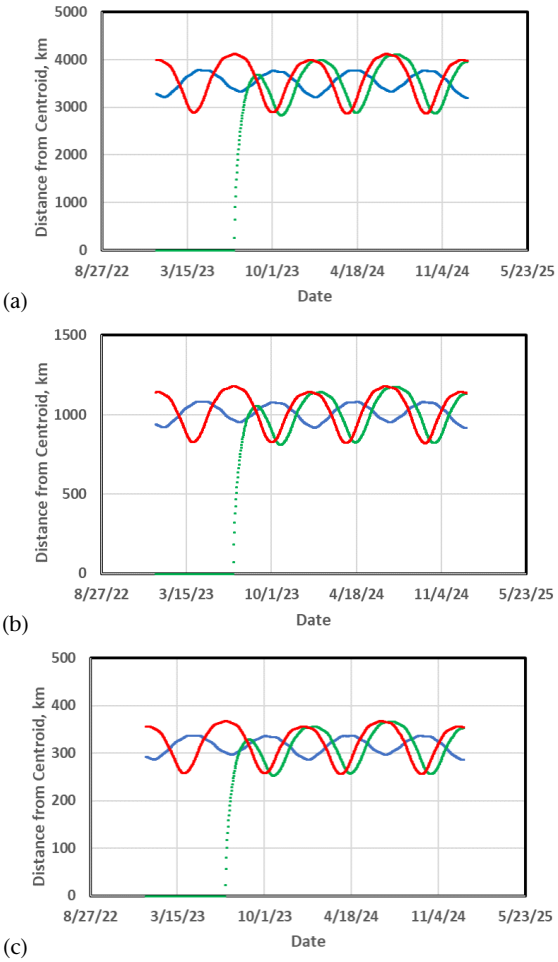

Figure 16. Permissible distances between L2 spacecraft so as to reside inside the uplink beamwidths for S-band (a), X-band (b), and K-band (c).

Legend:
JWST (red), Euclid (green), and GAIA (blue).

As one might expect, these do not seem to be too much different than for the case discussed for L1.

It is interesting that the Nancy Grace Roman Space Telescope, the expected successor to JWST, appears to be flying next to JWST on the same or a very similar trajectory [14].

C. Beamwidths at Lunar Distances

Shown in the "dart-board" graphic of Figure 17 are the "approximate" beamwidths for near-Earth uplink superimposed on the Moon; S-band half-power (blue circle), X-band half-power (green circle), K-band half-power (red circles), and S-band 10 dB down (dashed yellow circle).

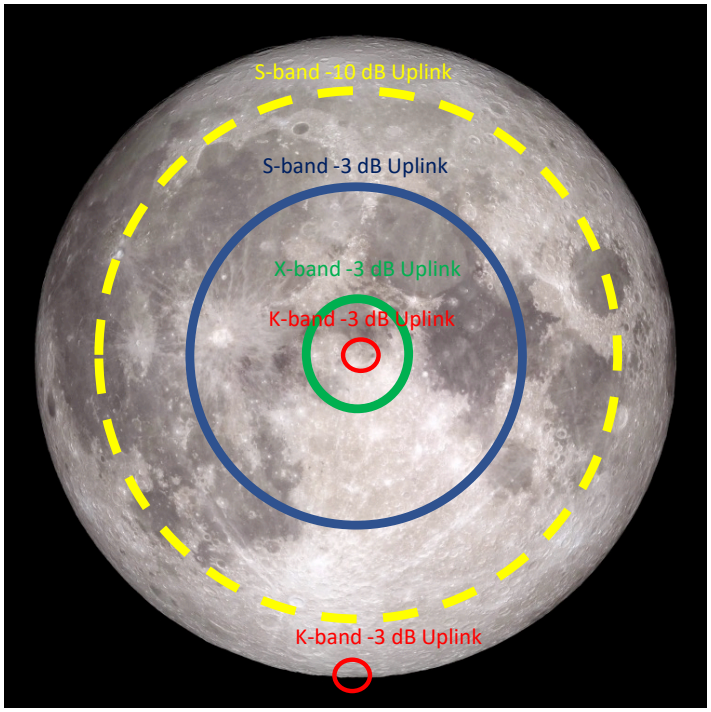

Figure 17. Image of Moon with various beamwidths superimposed.
Image Credit: NASA / GSFC / Arizona State University

Shown in Table 12 are S-band, X-band, and K-band uplink and downlink HPBW (3 dB down) beam parameters for a 34-m antenna at both minimum and maximum Earth–Moon distances for uplink (12a) and for downlink (12b). See Table 2 for a listing of link frequencies and HPBW assumptions for near-Earth frequency band allocations.

The K-band uplink beam spans about 152 km in extent (133 km for downlink). This would provide direct to Earth / direct from Earth MUPA and MSPA services at K-band to any assets located within 133 km of each other. Two prime sites for telecom relay (Malapert Mountain and Shackleton Crater rim) are located about 120 km from each other (Figure 18). The inserted red line in Figure 18 denotes the 120-km span between Malapert and

Table 12a. Uplink HPBWs at the Moon.

Lunar Distance (km)	Lunar Ang Extent (mdeg)	S-band Beamwidth / Lunar Diameters	X-band Beamwidth / Lunar Diameters	K-band Beamwidth / Lunar Diameters
360,000	553.06	0.486	0.139	0.044
405,696	490.77	0.548	0.157	0.050

Table 12b. Downlink HPBWs at the Moon.

Lunar Distance (km)	Lunar Ang Extent (mdeg)	S-band Beamwidth / Lunar Diameters	X-band Beamwidth / Lunar Diameters	K-band Beamwidth / Lunar Diameters
360,000	553.06	0.447	0.119	0.038
405,696	490.77	0.503	0.134	0.043

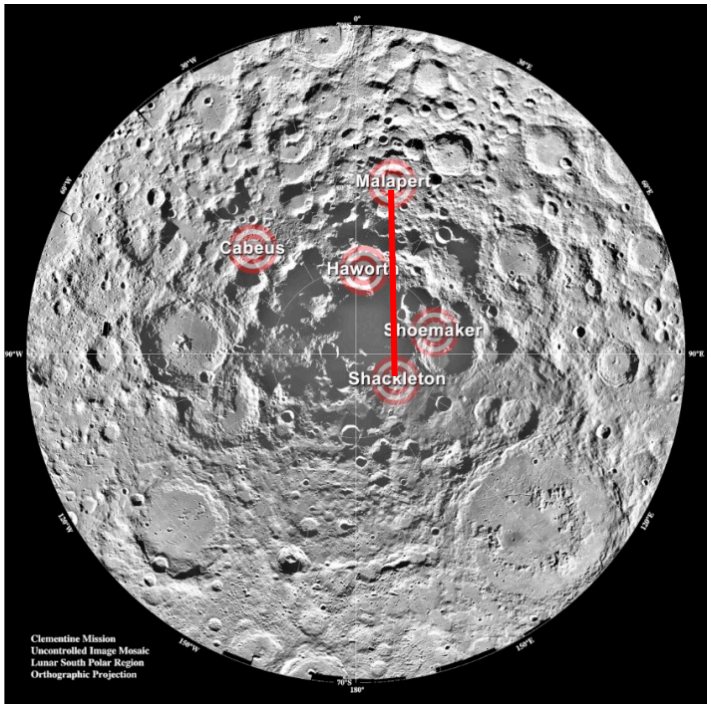

Figure 18. Depiction of lunar south pole with various surface features shown. Red line between Malapert and Shackleton denotes 120-km distance. Image Credit: NASA

Shackleton, which lies within the 133-km downlink span. Note that this is not an Earth-based direction projection, as it is used only to denote relative locations at the lunar South Pole. Thus, the apparent distance as seen from Earth would be much smaller. Various link considerations include elevation angle visibility masks at the site in question and visibility of the Earth station; an asset on the crater rim or mountain being able to communicate to a 34-m antenna on Earth; the fact that nights at the lunar South Pole can be as long as 7.5 Earth days, which is important for solar panel illumination issues [15]; and mitigation of multipath from lunar surface at very low-elevation angles.

Other considerations include the treatment of lunar hot body noise in link budgets. For a 34-m DSN antenna pointed at the center of the lunar disk, the increase in system noise temperature due to lunar hot body noise is as follows: for S-band, ~136 ± 1.4 K; for X-band, ~184.2 ± 5.6 K; and for K-band, ~166 ± 20 K [16]. When the beam center is pointed at the lunar rim, such as at the lunar South Pole, we have the increase in system noise temperature due to lunar hot body as follows: for S-band, ~70 K (43 K to 76 K); for X-band, ~83 K (50 K to 115 K); and for K-band, ~70 K (16 K to 138 K) [16]. It should be emphasized that the above measurements quoted for K-band (26 GHz) were actually taken at Ka-band (32 GHz) in Reference [16]. Note that there is a high variation in hot body noise with lunar phase angle for X-band and K-band, where at S-band it is essentially constant.

At S-band, multipath loss at the lunar surface involves typical fades of ~10 dB, and occasional deep fades of ~20 to ~25 dB that may occur at elevation angles below 12 deg. These numbers are "rule-of-thumb" and, in actuality, would depend on factors such as terrain topography and the directivity of the landed spacecraft's onboard antenna. No empirical data is yet available at X-band, so we assume 20 to 25 dB as a worst-case placeholder for now. At K-band, one could assume minimal loss if the main beam of the lunar surface antenna does not intersect with the surface (e.g., 0.75 deg for 1-m aperture).

D. Gateway

Figure 19 illustrates the Gateway link configurations to the various surface and orbital assets on or in the vicinity of Earth and the Moon. Gateway will use X-band and K26/K22-bands for direct-to-Earth links [17]. While the SpaceX human landing system (HLS; Starship) will use S- and K-bands, the Blue Origin HLS plans to use X- and K-bands. ESA's vehicles also appear to be gravitating toward X- and K-bands. A SOAP depiction of the Gateway orbit along with that of the Lunar Reconnaissance Orbiter (LRO) is shown in Figure 20. Note that the beamwidths at S-, X-, and K-bands have not been superimposed on Gateway in Figure 20, as they will lie comparable to or within the diameter of the Moon (Figure 17). Instead, we perform a "distance from Gateway" analysis as discussed below.

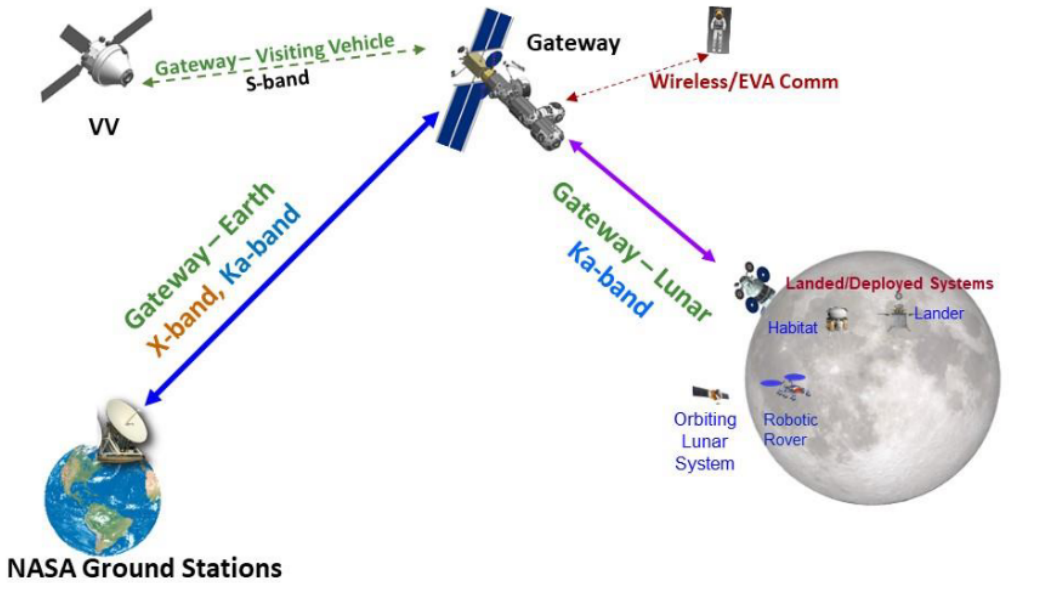

Figure 19. Depiction of Gateway along with the links to the various assets. Graphic courtesy of NASA from [17].

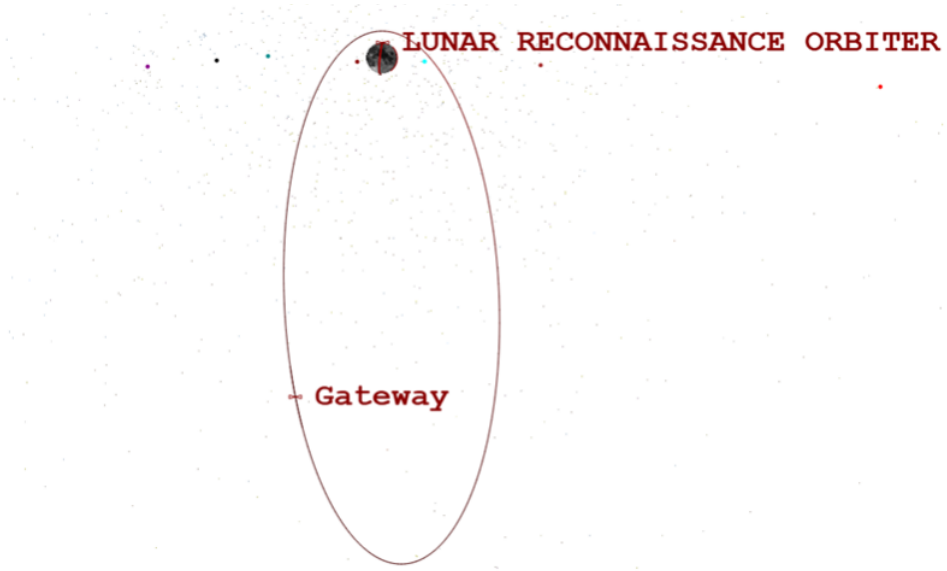

Figure 20. Depiction of the Gateway and LRO orbit relative to the Moon as seen from Earth (from SOAP).

Figure 21 depicts the distance (d) in km from any given asset (HLS, ESA, or Blue Origin) to Gateway that lies within the HPBW calculated as d = (HPBW/2) * R for each frequency band, where HPBW is in radians and range distance R is in km. Figure 22 displays the range distance from the Gateway to the 34-m Earth station.

Table 13 displays the minimum and maximum transverse distances of any in-beam assets to Gateway over the 2022–2035 period.

Table 13. Distances between Gateway and given asset.

Frequency Band	Minimum Distance (km)	Maximum Distance (km)
S-band	841	1,005
X-band	243	290
K-band	75	89

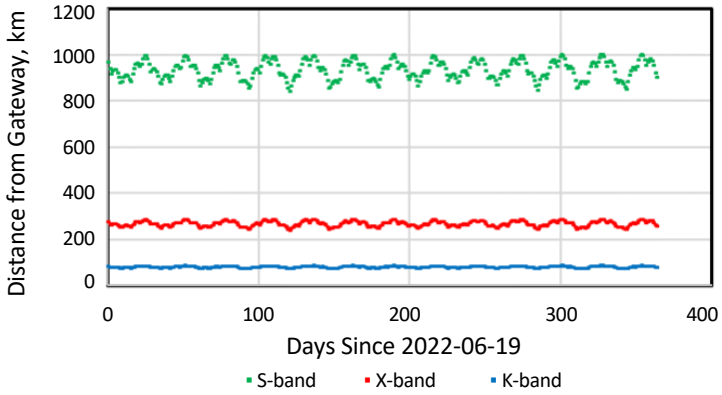

Figure 21. Minimum distance of any given asset within HPBW of Gateway during a one-year period at frequencies of interest; S-band (green), X-band (red), and K-band (blue).

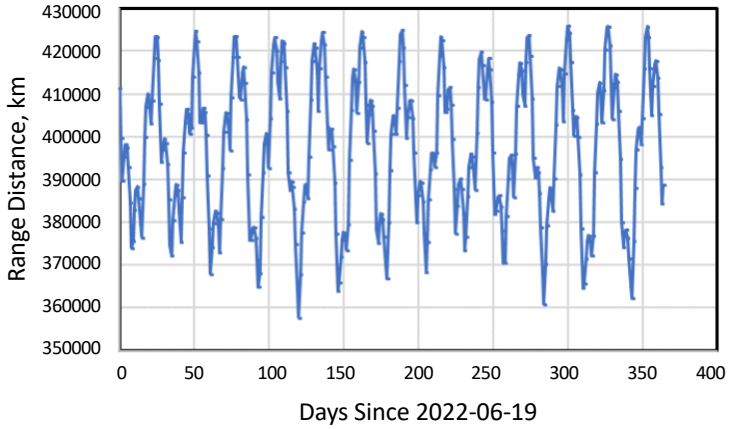

Figure 22. Gateway to Earth range distance.

IV. Concluding Remarks

The number of spacecraft that require support from NASA's DSN is expected to increase significantly beyond the current loading level within the next few years. Thus, NASA has been exploring ways to increase capacity using existing antennas. One way to do this is through beam-sharing. While successfully employed for simultaneous downlink, beam-sharing for simultaneous uplink using the same frequency band has not been an option. An approach to achieving near-simultaneous uplink involves multiplexing the data streams intended for all of the participating in-beam spacecraft onto a single uplink frequency. In this paper, we focused on examining the various near-Earth and interplanetary scenarios when multiple spacecraft are involved, and inspected the number of spacecraft that may fall within the beamwidth of a 34-m DSN station. The scenarios that we examined included planetary orbital spacecraft, the Sun–Earth Lagrange points at L1 and L2, the lunar vicinity, and the lunar Gateway. For this study, we considered cases involving S-band (2 GHz), X-band (7.1–8.4 GHz), K-band (22–27 GHz), and Ka-band (32–34 GHz). The results for these scenarios suggest that an abundance of in-beam opportunities exist for using MUPA in conjunction with MSPA to simultaneously support multiple spacecraft via a single antenna. By actively engineering for such opportunities during mission design, flight projects may be better positioned to obtain the DSN tracking they need when contention for antenna assets is growing.

Acknowledgments

The research was carried out at the Jet Propulsion Laboratory, California Institute of Technology, under a contract with the National Aeronautics and Space Administration (80NM0018D0004). We appreciate the support provided by Space Communications and Navigation (SCaN) system engineering. We also appreciate the support provided by Kristy Tran of the Jet Propulsion Laboratory in locating and delivering requested trajectory files.

References

[1] D. S. Abraham, S. E. Brys, J. L. Gao, S. Malhotra, L. Meshkat, D. D. Morabito, J. A. O'Dea, E. R. Pascua, M. Sanchez Net, D. K. Shin, and Z. Towfic, "Antenna beam-sharing: progress toward multiple uplinks per antenna," *17th International Conference on Space Operations,* SpaceOps-2023, ID # 139, March 6–10, 2023, Dubai, United Arab Emirates. https://spaceops2023.org/sopsprogramme/

[2] D. D. Morabito, Z. Towfic, and D. S. Abraham, "Comparison of type 2 versus type 3 carrier tracking loops under high dynamic signal conditions," *16th International Conference on Space Operations,* SpaceOps-2021,8,x1358 (Virtual) , May 3–5, 2021, Cape Town, South Africa.

[3] D. D. Morabito and D. S. Abraham, "Multiple uplinks per antenna (MUPA) signal acquisition schemes," *Space Ops 2018 Conference,* May 28–June 1, 2018, Marseille, France.

[4] D. S. Abraham, S. Malhotra, L. Meshkat, D. D. Morabito, J. A. O'Dea, E. R. Pascua, M. Sanchez Net, D. K. Shin, L. C. Stewart, and Z. J. Towfic, "Multiple uplinks per antenna (MUPA): where are we now?" Presentation at *Interplanetary Small Satellite Conference,* April 30–May 2, 2024, University of Arizona, Tucson, Arizona.

[5] D. Y. Stodden and G. D. Galasso, "Space system visualization and analysis using the satellite orbit analysis program (SOAP)." In *Proceedings of the 1995 IEEE Aerospace Applications Conference,* February 4–11, 1995, Aspen, Colorado. http://ieeexplore.ieee.org/stamp/stamp.jsp?arnumber=00468892

[6] S. D. Slobin, "34-m BWG stations telecommunications interfaces." In *DSMS Telecommunications Link Design Handbook,* Doc. 810-005, Module 104, Rev. O, Jet Propulsion Laboratory, California Institute of Technology, Pasadena, California, 2022.

[7] S. E. Smreker et al. "VERITAS (Venus Emissivity, Radio science, InSAR, Topography, And Spectroscopy): a Discovery mission," 978-1-6654-3760-8/22/$31.00 © 2022 IEEE. https://smd-cms.nasa.gov/wp-content/uploads/2023/07/VERITAS_Paper_010622_with_copyright_info.pdf

[8] H. Svedhem, D. Titov, F. Taylor, O. Witasse, "Venus express mission," *Journal of Geophysical Research: Planets*, vol. 114(e5), May 2009. https://doi.org/10.1029/2008JE003290

[9] M. Sekerak, et al., "The Deep Atmosphere Venus Investigation of Noble gases, Chemistry and Imaging (DAVINCI) mission: flight system design technical overview," *2022 IEEE Aerospace Conference (AERO),* pp. 1–11, Big Sky, Montana, USA. https://doi.org/10.1109/AERO53065.2022.9843454

[9b] DAVINCI https://nssdc.gsfc.nasa.gov/nmc/spacecraft/display.action?id=DAVINCI-P

[10] Rocket Lab site: https://www.rocketlabusa.com/missions/upcoming-missions/first-private-mission-to-venus/

[11] R. French, C. Mandy, R. Hunter, E. Mosleh, D. Sinclair, P. Beck, S. Seager, J. J. Petkowski, C. E. Carr, D. H. Grinspoon, and D. Gaumgardner, "Rocket lab mission to Venus," *Aerospace* vol. 9, no. 8, p. 445. https://doi.org/10.3390/aerospace9080445

[12] S. D. Slobin, "Atmospheric and environmental effects." In *DSMS Telecommunications Link Design Handbook,* Doc. 810-005, Module 105, Rev. E, Jet Propulsion Laboratory, California Institute of Technology, Pasadena, California, 2015.

[13] J. S. Parker, R. Lillis, S. Curry, C. Ott, A. Kohler, and M. Rosen, "EscaPADE: a low-cost formation at Mars." In *73rd International Astronautical Congress (IAC),* IAC-22-B4,IP,23,x74203, September 18–22, 2022, Paris, France.

[14] Roman Telescope (RST), accessed July 23, 2024. https://www.euronews.com/next/2023/03/19/nasas-roman-telescope-how-james-webbs-successor-will-map-universe-with-colossal-amounts-of

[15] C. H. Lee and K.-M. Cheung, "Complete lunar exploration coverage analysis," *The Interplanetary Network Progress Report,* vol. 42-175, Jet Propulsion Laboratory, Pasadena, California, pp. 1–30, November 15, 2008. https://ipnpr.jpl.nasa.gov/progress_report/42-175/175F.pdf

[16] D. D. Morabito, "Lunar noise-temperature increase measurements at S-band, X-band, and Ka-band using a 34-meter-diameter beam-waveguide antenna" *The Interplanetary Network Progress Report,* vol. 42-166, Jet Propulsion Laboratory, Pasadena, California, pp. 1–18, August 15, 2006. https://ipnpr.jpl.nasa.gov/progress_report/42-166/166C.pdf

[17] R. Dendy, D. Zeleznikar, and M. Zemba, "NASA lunar exploration – gateway's power and propulsion element communications links," *38th International Communications Satellite Systems Conference (ICSSC) / 26th Ka-band Conference,* September 27–30, 2021, Arlington, Virginia, USA. https://www.kaconf.com/2021/